Subtle Differences in System Noise Measurements and Calibration of Noise Standards*

T. MUKAIHATA†, B. L. WALSH, JR.‡, MEMBER, IRE, M. F. BOTTJER†, AND E. B. ROBERTS†

Summary—Stringent system requirements and the lack of accurate standards have been the source of many controversies in low-noise receiver measurements.

Some of the critical measurement problems where subtle errors commonly arise, and their significance in automatic noise temperature monitoring systems have been investigated at L-, S-, and X-band frequencies.

Problems of interest include the following: 1) difficulty in determining losses associated with low-noise systems and measuring equipment, 2) differences in noise figure measurements depending upon the use of gated or nongated receivers, 3) discrepancies in excess noise ratios of secondary standard argon gas tubes, 4) nonuniformity in the output noise power of such gas tubes due to critical coupling from the gas tube proper to the waveguide (or coaxial) output flange.

As a partial solution to these problems noise standards at liquid nitrogen temperature in coax and waveguide were developed at the aforementioned bands.

I. Introduction

THE TECHNICAL "know how" and engineering skill in the fabrication of parametric amplifiers (paramps) and other low-noise devices have advanced to such a state that there is considerable demand for adapting such devices as subsystems to complicated existing radar, deep space probe, and communication systems. In addition, an accurate automatic technique for continuous monitoring of noise figure of a system has become a significant requirement.

The Deep Space Instrumentation Facility (DSIF) Paramp Subsystem was developed with provisions to meet the above requirement at *L*- and *S*-band frequencies by the Microwave Components Department, Aerospace Group, for the Jet Propulsion Laboratory, a prime contractor of NASA.

The paramp subsystem utilizes a paramp and associated temperature control and power-source equipment for providing stable, low-noise RF amplification of incoming signals from the antenna feed line. The automatic system excess noise temperature (ASENT) measurement equipment is included to provide continuous measurement of system temperature of the receiver system by comparing total noise power referred to the input of the paramp with calibrated noise power injected into the system.

The scope of this paper is confined to the problems associated with the calibration of the ASENT equipment, calibration of the gas tube standard incorporated in the system, and noise-figure measurements of the paramp subsystem. A prime concern is the accuracy involved in measurement of low-noise-figure receivers and the calibration of pulsed gas tube noise generators.

II. Description and Operating Principle of Paramp Subsystem

The ASENT equipment provides an indication of the total system noise temperature during actual tracking operations. For example, in radio astronomy application the ASENT equipment provides an indication of the noise produced by the signal source at the receiver input, plus the antenna feed line loss, plus the noise produced within the receiver.

The total system noise temperature is obtained by automatically comparing the actual system noise with periodically injected calibrated noise signal (96°K) through a nominal 20-db coupler (see Fig. 1). The receiver is periodically gated to sample the total system noise with the noise source alternately pulsed on and off. The sampled pulse for the gas tube fired and unfired conditions are designated as N_2 and N_1, respectively. The power ratio of the integrated values of N_2 and N_1, as analyzed by the circuit, provide the system noise temperature.

The sampling for the fired condition of the gas tube is made during the constant ionization period rather than during the gas tube ionization build-up or decay time. The triggering pulse for the gated receiver was 250-μsec wide at 300 pps in order to sample the fired and unfired conditions of the gas tube which was periodically fixed at 150 pps.

III. Reference Standards

A. Coaxial Cold Load

At the outset of the DSIF program, a coaxial noise standard was needed for the calibration of argon gas tubes which were to be incorporated as secondary noise standards in the paramp subsystems. A coaxial noise standard was developed with the idea of using a single load to be used at two known reference temperatures. This was believed to be an advantage over the construction of two loads with similar characteristics but at different temperatures. It was also intended to avoid the use of a coaxial switch (due to repeatability problem) in switching from one load to another.

An inverted tapered coaxial load was used to assure good physical contact with its casing which was im-

* Received June 4, 1962; revised manuscript received August 2, 1962.

† Primary Standards Laboratory, Microwave Section, Aerospace Group, Hughes Aircraft Company, Culver City, Calif.

‡ Microwave Components Department, Aerospace Group, Hughes Aircraft Company, Culver City, Calif.

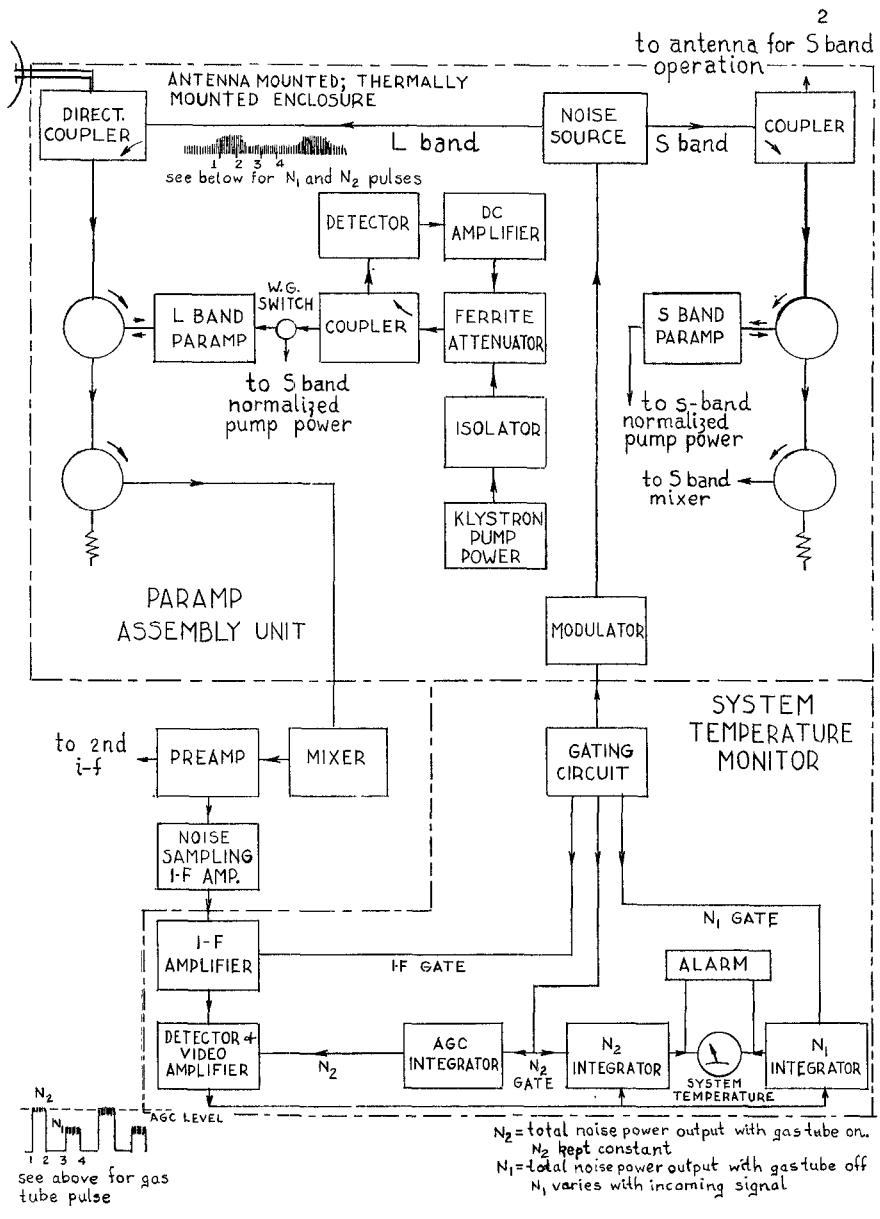

Fig. 1—Block diagram of DSIF paramp subsystem.

mersed in liquid nitrogen. Both ends of the casing extended through and beyond the insulated liquid-nitrogen container. The section of the casing containing the load was centered in the liquid nitrogen supply. A type N connector was placed on one end to connect to the system under test. The other end was made so that the center conductor was accessible. The use of a conventional coaxial switch was avoided by making the center conductor removable from the type N connector by pulling the center conductor from the accessible end. Upon disconnecting the center conductor an open-circuit condition (lossless discontinuity) would cause the noise power generated in an isolator preceding the cold load to be reflected into the receiver input. The temperature of the load at the center was measured to be $77.5° \pm 0.2°$K with a platinum resistance thermometer, certified by NBS to liquid oxygen temperature ($-182.970°$C). The data was extrapolated to liquid nitrogen temperature.

A commercial hot-cold body standard noise generator became available later and extensive comparisons with similar models and with the aforementioned cold load as well as with another cold load made by C. T. Stelzrid of JPL revealed no differences larger than the measurement accuracy of ± 0.05 db.

The temperature of the hot load (373.1°K) was verified by repeated comparison of noise-figure measurements and calibration of gas tube noise sources made with the hot-cold body standard and the Hughes cold-load standard. The results of this comparison indicated a negligible error. In addition the temperature measurement of ice water and of a dry-ice acetone solution required knowledge of the hot temperature. The results are given in Section V-B.

The coaxial switch in the commercial unit exhibited a loss of 0.03 db with a high degree of repeatability in measurement in switching from hot to cold load. The VSWR of the hot-cold body standard was 1.08 or less

at 0.96, 1.3, and 2.295 Gc with essentially no VSWR difference between the hot and cold loads. For the systems under consideration, sufficient isolation existed in the paramp circulator so that the slightly mismatched source did not produce any noticeable error. Since the losses between the standard cold load at 77.3°K (theoretical) and the input terminal of the system at temperature t_n (approximately 293°K) was of the order of 0.01 db, the error due to temperature gradient has been neglected. A first-order approximation can be made by postulating a linear temperature rise with guide length from the system input temperature which is at t_n and by integrating the temperature rise per unit guide length over the length. If the resistive loss in the guide walls is appreciable and the temperature difference between the source and the system is large, a correction for the effective source temperature can be made as computed by Sees [1] and Wells, Daywitt, and Miller [2]. Computations gave a value of 78°K for the reference cold temperature.

B. Waveguide Cold Load

A waveguide cold load was constructed by placing two conventional pyramidal loads in the corners of the waveguide casing to obtain maximum contact of the loads with the waveguide walls. An epoxy potting compound was used to hold the loads in place and to seal the end of the load casing. The load thus constructed has a VSWR of less than 1.01 at both room temperature and when cooled by liquid nitrogen. Large radiating fins were mounted near the output flange of the cold load, and a fan was directed onto the fins in order to limit the region of temperature gradient between the cold source and the system. A mica window was placed at the output flange to prevent condensation of moisture inside the guide. The VSWR, due to the mica, increased to 1.05. For systems sensitive to slightly mismatched source, it is recommended that an isolator be inserted between the source and the system. A conventional waveguide switch was used for switching either a matched load at room temperature or the cold load into the circuit.

IV. Procedure and Analysis

The technique utilized in determining noise figure and excess-noise ratio of a gas tube is the conventional IF attenuator method in which the Y factor is obtained. Figs. 2 and 3 actually represent a single system under different conditions for determining the noise figure and the excess-noise ratio of a gas tube, respectively. Essentially, two Y factor measurements are made. The first Y factor measurement (Fig. 2) determines the noise factor f or the effective temperature t_e of the receiver by keeping the gas tube unfired and adjusting the IF attenuator in the receiver for equal IF output when S_1 is switched from hot to cold load (or vice versa).

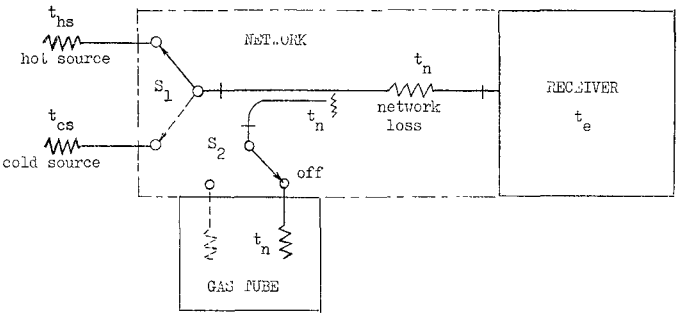

Fig. 2—A simplified diagram of system temperatures involved in determining the noise figure or effective temperature t_e of a receiver.

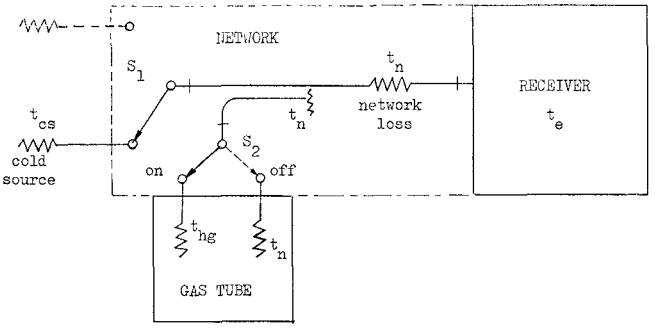

Fig. 3—A simplified diagram of system temperatures involved in determining the excess-noise ratio of a gas tube noise source.

The noise figure or effective temperature is calculated by use of the appropriate equation, as derived in the analysis. The second Y factor or Y' measurement (Fig. 3) determines the excess-noise ratio of a gas tube from the measured noise factor of the receiver. This is accomplished by connecting S_1 to a standard temperature and obtaining equal IF output by adjusting the IF attenuator for the fired and unfired conditions of the gas tube. (Preferably, S_1 is connected to the cold temperature in order to obtain a larger Y factor which results in a smaller error.) The excess-noise ratio is calculated from the appropriate equation also derived in the analysis. The stability of the paramp under test was assured by use of a stabilized pump power source and regulated bias supply for the varactor in the paramp. The tests were conducted under constant ambient temperature condition. A 30-Mc IF attenuator calibrated within 0.02 db of an NBS transfer standard was also used.

The definitions used in the following analysis are

t_{hs} = hot-source temperature,
t_{cs} = cold-source temperature,
t_n = network temperature,
τ is the transmission coefficient defined in db as $A = 10 \log 1/\tau$,
c is the coupling coefficient defined in db as $C = 10 \log 1/c$,
a is the absorption coefficient defined as $a = 1 - c - \tau$ where $D = 10 \log 1/a$.

Parameters τ, c, and a are calculated from measurements of attenuation A and coupling-factor C of the network. A well-matched system is assumed and higher-order terms beyond the accuracy of measurements are omitted in the analysis.

A. Receiver Effective Temperature

The following standard definitions are used with reference to Fig. 2.

$$y = \frac{t_e + t_{2h}}{t_e + t_{1c}}, \tag{1}$$

$$t_e = (f - 1)290. \tag{2}$$

t_{2h} = Total temperature at the receiver-input terminal with switch S_1 connected to the hot source at temperature t_{hs} and S_2 connected to the unfired gas tube terminated in a matched load at ambient network temperature t_n (Fig. 2).

t_{1c} = Total temperature at the receiver-input terminal with S_1 connected to the cold source at temperature t_{cs} and S_2 remaining at t_n.

t_e = Effective receiver-noise temperature, referred to the receiver input.

1) Noise Figure of Receiver with Hot and Cold Body Standard Temperatures Applied: Solving (1) for the effective receiver temperature:

$$t_e = \frac{t_{2h} - yt_{1c}}{y - 1}, \tag{3}$$

$$t_e = t_{2h} - 2t_{1c} \qquad \text{3-db method.} \tag{3a}$$

The total temperature at the receiver input with S_1 switched to the hot and cold source, respectively, is

$$t_{2h} = (t_{hs} - t_n)\tau + t_n, \tag{4}$$

$$t_{1c} = (t_{cs} - t_n)\tau + t_n. \tag{5}$$

From (1) and (2), the noise factor becomes

$$f = \frac{e_h + ye_c}{y - 1}, \tag{6}$$

$$f = e_h + 2e_c \qquad \text{3-db method} \tag{6a}$$

where

$$e_h = \frac{t_{2h}}{290} - 1, \tag{7}$$

$$e_c = 1 - \frac{t_{1c}}{290} \qquad t_{1c} < 290°\text{K}. \tag{8}$$

The corresponding noise figure F in decibels is

$$F = 10 \log (e_h + ye_c) - 10 \log (y - 1), \tag{9}$$

$$F = 10 \log (e_h + 2e_c) \qquad \text{3-db method.} \tag{9a}$$

2) Noise Figure of Receiver Using a Cold Body Standard: With reference to Fig. 2 and $t_{hs} = t_n$, and $e_h = 0$, the following equations apply:

$$t_e = \frac{t_n - yt_{1c}}{y - 1}, \tag{10}$$

$$t_e = t_n - 2t_{1c} \qquad \text{3-db method,} \tag{10a}$$

$$f = \frac{ye_c}{y - 1}, \tag{11}$$

$$f = 2e_c \qquad \text{3-db method.} \tag{11a}$$

In decibels

$$F = 10 \log y + E_{cs} - A - 10 \log (y - 1), \tag{12}$$

$$F = 3 + E_{cs} - A \qquad \text{3-db method} \tag{12a}$$

where

$$E_{cs} = 10 \log e_{cs} \tag{13}$$

$$e_{cs} = 1 - \frac{t_{cs}}{290}; \qquad t_{cs} < 290°\text{K}.$$

B. Calibration of the Gas Tube

If the gain and the system parameters remain constant, then consecutive Y and Y' measurements can be made in accordance with the described procedure. The two measurements are interrelated through the effective temperature relation of (1) as follows:

$$\frac{t_{2h} - yt_{1c}}{y - 1} = \frac{t_{2h} - y't_{1c}'}{y' - 1}. \tag{14}$$

The unprimed and primed letters refer to measurement conditions in determining the noise figure and excess-noise ratio of the gas tube, respectively. Under the conditions of Fig. 3, the following temperatures exist at the receiver input:

$$t_{2h}' = (t_{cs} - t_n)\tau + (t_{hg} - t_n)c + t_n, \tag{15}$$

$$t_{1c}' = (t_{cs} - t_n)\tau + t_n. \tag{16}$$

t_{2h}' and t_{1c} are determined from (4) and (5).

1) Calibration of Gas Tube with Hot and Cold Body Standard: From (14) the excess-noise ratio of the gas tube e_{hg} can be derived as

$$e_{hg} = \frac{(y' - 1)(e_{hs} + e_{cs})\tau}{c(y - 1)} = \frac{(y' - 1)(t_{hs} - t_{cs})\tau}{c(y - 1)290}, \tag{17}$$

$$e_{hg} = \frac{(t_{hs} - t_{cs})\tau}{290c} \qquad \text{3-db method} \tag{17a}$$

where

$$e_{hg} = \frac{t_{hg}}{290} - 1; \qquad e_{hs} = \frac{t_{hs}}{290} - 1; \qquad e_{cs} = 1 - \frac{t_{cs}}{290}.$$

In decibels,

$$E_{hg} = C + 10 \log (y' - 1) + 10 \log \frac{(t_{hs} - t_{cs})}{290} - 10 \log (y - 1) - A. \tag{18}$$

2) Calibration of Gas Tube with a Cold Body Standard: For the condition $t_{hs} = t_n$, $e_{hs} = 0$, and the following equations apply:

$$e_{hg} = \frac{\tau(y' - 1)e_{cs}}{c(y - 1)}, \tag{19}$$

$$e_{hg} = \frac{\tau e_{cs}}{c} \quad \text{3-db method,} \tag{19a}$$

$$E_{hg} = C - A + 10 \log (y' - 1) - 10 \log (y - 1) + 10 \log \left(1 - \frac{t_{cs}}{290}\right), \tag{20}$$

$$E_{hg} = C - A + 10 \log \left(1 - \frac{t_{cs}}{290}\right) \text{ 3-db method.} \tag{20a}$$

V. Measurements

A. Noise Figure Measurements and Calibration of Gas Tubes

Using a pulse with a 50 per cent duty cycle, fast rise-and-fall time characteristics, and minimum overshoot, one would expect a 3-db difference in a 30-Mc receiver output as compared to the receiver output with a gas tube fired continuously. Fig. 4 shows a typical condition of the ionization and deionization characteristics. Also, the symmetry of the modulating waveform is an important consideration. For these reasons a gated receiver which samples the fired and unfired noise temperatures during completely ionized and deionized states is recommended.

Measurements using a paramp were first made at 1.3 Gc. The measured excess-noise ratio of the argon gas tube was 15.9 db. Noise-figure measurements on the prototype paramp subsystem were made with an argon gas tube with an advertised value of 15.2 db. Noise figures as low as 0.2 and 0.8 db were obtained at 0.96 and 2.295 Gc, respectively. These results were compared with manual measurements utilizing a commercial hot- and cold-load noise standard. A discrepancy between the manual and automatic measurements was found. Extensive tests indicated that the gas tube excess-noise ratio was greater than 15.2 db.

Test results at 2.295 Gc are given in Table I. A difference in excess-noise ratio amounting to 1 db was found. This was attributed to the critical mechanical alignment of the gas tube with respect to the coaxial coupling circuit.

Measurements made at 0.96 Gc on the same gas tubes gave a higher average value of excess-noise ratio of 16.0 ± 0.1 db. Typical values of cold loss A_c and hot loss A_h were 0.1 and 25 db, respectively. The values at 2.295 Gc were $A_c = 0.4$ db and $A_h = 19$ db. An approximation of the internal gas tube temperature t_{hg} relative to the measured gas tube temperature $t_{hg(\text{apparent})}$ at the output connector is given by

$$t_{hg(\text{apparent})} = t_{hg}(1 - A_h)A_c, \tag{21}$$

where $t_{hg(\text{apparent})} = t_{hg}$ in Table I.

The room temperature correction has been neglected in (21). The internal apparent temperature is calculated to be $t_{hg} = 12{,}500°\text{K}$ for $t_{hg(\text{apparent})} = 12{,}220°\text{K}$ at 0.96 Gc. Since the same tube was used at 0.96 and 2.295 Gc, t_{hg} at 2.295 Gc was calculated from (21) using $t_{hg} = 12{,}500°\text{K}$ and the appropriate cold and hot losses. The computed apparent value $t_{hg(\text{apparent})} = 11{,}400°\text{K}$ is in good agreement with the data of Table I.

On the basis of the average values determined for the noise temperature of the gas tube, the nominal 20-db coupling value required an adjustment in order to inject the required reference 96°K into the system. The selection of 96°K was based on the following reasons:

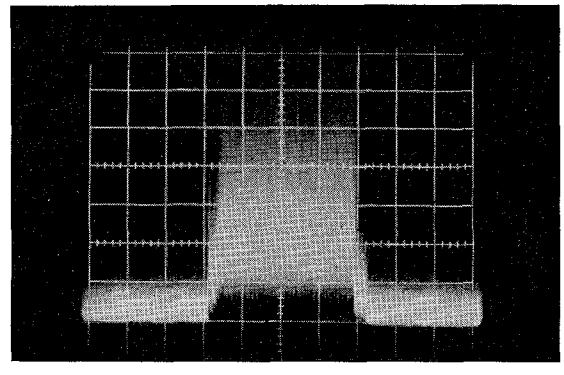

Fig. 4—Ionization buildup and decay characteristics of an argon gas tube.

TABLE I
Coaxial Gas Tube Calibration Data

Tube Serial No.	t_n (°K)	Y (db)	Y' (db)	t_e (°K)	t_{hg}* (°K)	E_{hg} (db)
130	298.2	2.40	5.98	256.2	11,382	15.83
134	298.2	2.54	6.29	230.6	11,606	15.91
157	296.0	2.54	5.58	230.6	9,376	14.96
173	296.0	2.44	6.17	248.6	11,794	15.98
157**	298.0	2.67	6.42	203.3	11,176	15.74
173**	298.0	2.63	6.37	207.6	11,233	15.77

* Numerical digits carried out for purposes of calculation.
** Tube nos. 157 and 173 interchanged in their respective casings.
Tube type: Bendix No. TD72; tube current = 150 ma; test conditions: $A = 0.55$ db; $C = 10.2$ db; $t_{cs} = 78°\text{K}$; $t_{hs} = 373°\text{K}$; frequency = 2.295 Gc.

1) The use of a nominal 20-db coupler with an anticipated excess-noise ratio of 15.2 db for the argon tube.
2) The resolution and sensitivity of the pulse ratio system at the system temperatures expected.
3) The prevention of obscuring weak signals during system temperature measurements.

A total of seven paramp subsystems were developed and evaluated. The noise figures ranged from 1.2 db to 2.2 db at 0.96 Gc and 2.295 Gc.

B. Measurement of Standard Temperatures

In order to obtain consistent measurements, a calibrated gas tube was used to determine the temperature of other liquids which were substituted for the liquid nitrogen. The standard hot source temperature in conjunction with the calibrated argon tube was used to determine the unknown cold temperature. The relationship between measured quantities and the unknown cold temperature is given by

$$t_{cx} = t_{hs} - \frac{c(y-1)(t_{hg}-t_n)}{y(y'-1)}. \tag{22}$$

With the container for the cold load filled with water and ice, the following data was obtained at 0.96 Gc:

$Y = 0.900$ db $\quad A = 0.44$ db $\quad t_{hg} - t_n = 11{,}920°\text{K}.$

$Y' = 4.830$ db $\quad C = 10.84$ db.

The ice-water temperature was determined from (22) as

$$t_{\text{ice water}} = 373°\text{K} - \frac{0.230(1094°\text{K})}{(2.041)(1.230)} = 272.9°\text{K}.$$

Dry-ice and acetone mixture was also measured. The values for Y and Y' were 1.700 and 4.600 db, respectively. The temperature was found to be

$$t_{\text{dry ice+acetone}} = 373°\text{K} - \frac{0.479(1094°\text{K})}{(1.938)(1.479)} = 190.5°\text{K}.$$

A thermocouple and bridge were used to measure the temperature of the mixture, and a reading of $190 \pm 1°\text{K}$ was obtained.

C. The Calibration of the System Temperature Monitor

The System Temperature Monitor (STM) is the system noise temperature indicating device of the ASENT equipment. It measures the pulse amplitude ratio of two pulses, N_2 to N_1, which are generated when the gas tube is turned on and off by the STM. The N_2 pulse represents a specified amount of calibrated noise power from the gas tube plus the receiver generated noise power at the receiver output. The N_1 pulse represents the amplified thermal noise at the receiver input plus the receiver generated noise.

Fig. 5 depicts the STM meter reading in terms of the pulse-amplitude ratio of N_2 to N_1. The equation which the STM meter responds to is as follows:

$$\text{PR}_{(\text{db})} = 10 \log_{10}\left(1 + \frac{96°}{t_m}\right) \tag{23}$$

where $PR_{(\text{db})}$ is the pulse amplitude ratio in db, t_n is the meter reading in degrees Kelvin which includes the source and receiver temperatures.

The block diagram of Fig. 6 depicts the equipment set up for the calibration of the STM. The calibration procedure is a modification of Hewlett-Packard's technique in the calibaration of HP automatic noise-figure meters. Various conditions of modulating pulse were investigated. Few of the common occurrences are depicted in Fig. 7. The relationship of the various waveforms are shown in Fig. 8.

D. Measurement of X-Band Gas Tubes

Table II gives the data for a series of measurements made on 10 different gas tubes using an X-band paramp at 9.25 Gc.

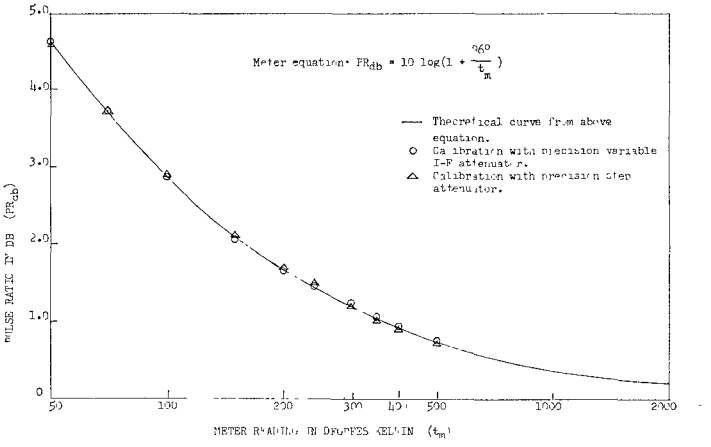

Fig. 5—System temperature monitor meter equation and calibration data.

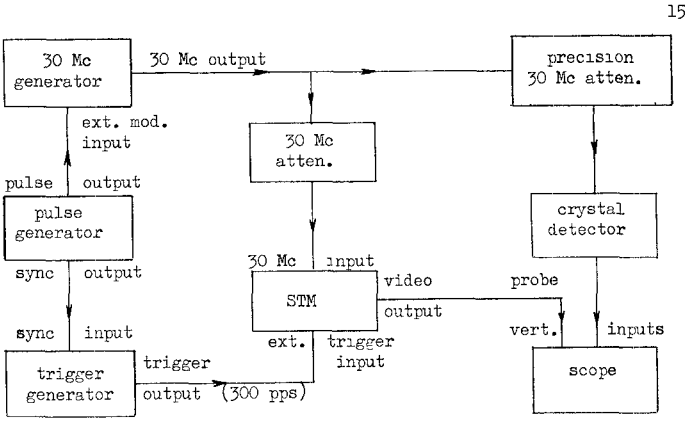

Fig. 6—A block diagram of the calibration setup for the system temperature monitor.

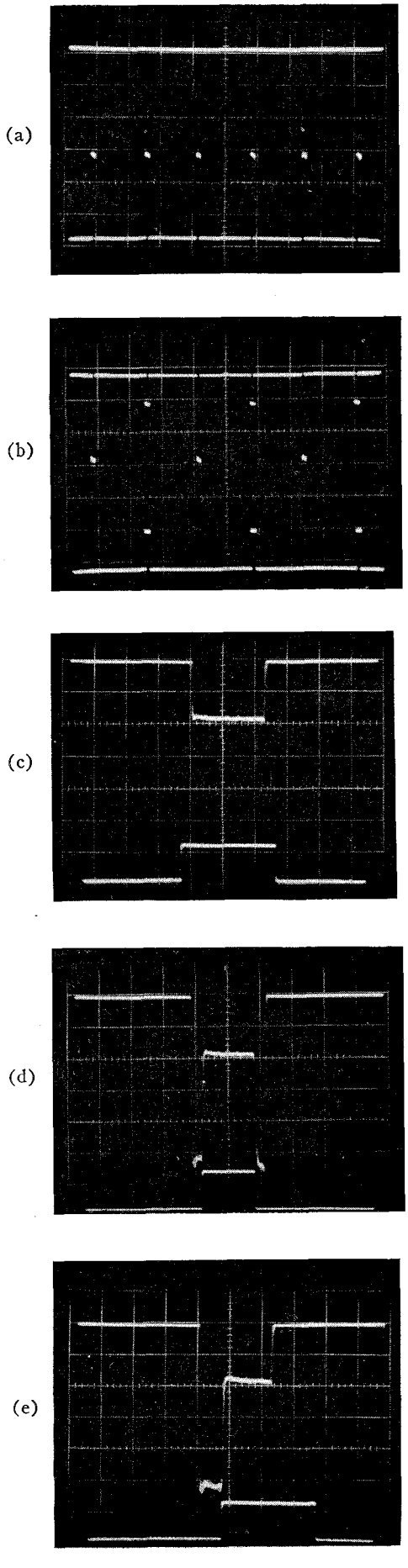

Fig. 7 (*Left*)—(a) Video output of STM with a 30-Mc CW input signal (upper trace). Detected 30-Mc input signal level (lower trace). (b) Video output with pulse modulated 30-Mc input showing N_2 and N_1 pulses (upper trace). Detected pulse modulated 30-Mc input signal (lower trace). (c) Expansion of N_2 pulse (upper trace) with the detected pulse modulated 30-Mc input signal (lower trace) adjusted for proper width and delay relative to N_2 pulse. (d) Expansion of N_2 pulse (upper trace) with insufficient width of modulating pulse (lower trace). (e) Expansion of N_2 pulse (upper trace) with improper delay of modulating pulse (lower trace).

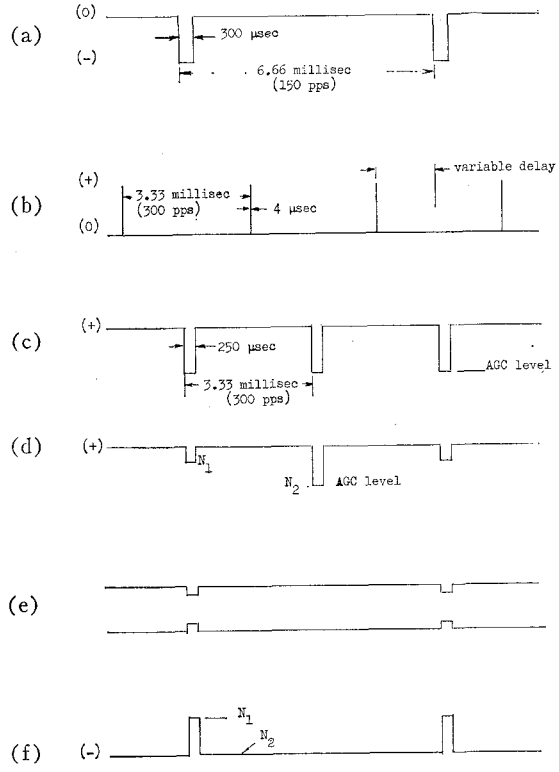

Fig. 8—(a) Output of the pulse generator which modulates the 30-Mc generator. (b) Output of the trigger generator which triggers the STM. (c) Video output pulse of the STM with a 30-Mc CW input. (d) Same video output pulse with the 30-Mc input pulse modulated. (e) Pulse modulated output of the 30-Mc generator. (f) Output of the crystal detector showing the detected modulation.

TABLE II

X-Band Gas Tube Calibration Data

Gas Tube (Ser. No.)	t_n (°K)	Y (db)	Y' (db)	t_e (°K)	t_{hg} (°K)	E_{hg} (db)
M-0750	305.0	1.02	4.03	547.0	10,893	15.63
M-0751	305.0	1.02	4.00	547.0	11,015	15.68
M-0752	304.3	1.09	4.28	496.3	11,178	15.74
M-0753	304.4	1.10	4.22	489.9	10,830	15.60
150	305.0	1.02	4.05	547.0	11,096	15.71
193	304.3	1.10	4.23	489.9	10,869	15.62
195	304.3	1.10	4.22	489.9	10,830	15.60
201	304.3	1.07	4.23	509.7	11,208	15.76
202	304.3	1.11	4.22	483.5	10,720	15.56
204	304.3	1.10	4.25	489.9	10,947	15.65

Tube type = Bendix No. TD41; tube current = 200 ma; test conditions: $A = 1.05$ db; $t_{cs} = 78$°K; $t_{hs} = t_n$; frequency = 9.25 Gc; E_{hg}(ave.) = 15.66 db.

VI. Error Analysis

Accuracies in noise-figure measurements and calibration of gas tube noise generators are limited by the following factors:

1) Mismatch errors.
2) Uncertainty in the standard temperature values.
4) System uncertainty due to gain instability, receiver nonlinearity, and spurious responses.
4) Error and repeatability in attenuation measurements for determining the Y factor and system coefficients such as τ, c, and a.

Mismatch errors can be minimized by use of tuners. However, the loss of the tuner must be considered. System mismatches can be a serious problem especially in coax and in situations where space limitation in packaging impose severe restrictions in component design. The mismatch case is treated in the Appendix.

In order to determine the extent of error introduced by the system mismatches, the following tests can be made:

1) The mismatch effect looking from the paramp to the antenna can be measured by use of a reflectometer technique. A signal generator and detector can be substituted for the circulator matched load and paramp, respectively. A short circuit is placed at the circulator input to establish a reference level. The short is then replaced by the system under test preceding the circulator. A return loss measurement (corrected for the insertion loss of the circulator) would be indicative of the desired effective reflection coefficient of the system. A large return loss value is indicative of a small error due to reflection.
2) The mismatch effect looking from the antenna input towards the paramp can be measured by noting the attenuation from the antenna feed line to the paramp. A minimum attenuation is desired in this case. However, the dissipative as well as the reflective losses are included in this measurement.

The other uncertainties mentioned above are treated in the following analysis.

A. *Noise-Figure Measurements by Use of Hot-Cold Body Standard*

Eq. (6) can be written as

$$F = 4.34(\ln_e(e_h + ye_c) - \ln_e(y - 1)) \tag{24}$$

where e_h and e_c are given by (7) and (8):

$$t_{2h} = (t_{hs} - t_0)\tau + t_0 \quad \text{and} \quad t_{1c} = (t_{cs} - t_0)\tau + t_0.$$

Let $u = e_h + ye_c = u(e_h, e_c, y)$; then

$$dF = 4.34\left(\frac{du}{u} - \frac{dy}{y - 1}\right) \tag{25}$$

where

$$du = \frac{\partial u(e_h, e_c, y)}{\partial e_h} de_h + \frac{\partial u(e_h, e_c, y)}{\partial e_c} de_c + \frac{\partial u(e_h, e_c, y)}{\partial y} dy$$

$$= de_h + y de_c + e_c dy. \tag{26}$$

Omitting negligible terms,

$$de_h \approx \frac{\partial e_h}{\partial t_{2h}} dt_{2h} = \frac{1 + \tau dt_{hs} - \tau dt_0 + (t_{hs} - t_0)d\tau}{t_0}, \tag{27}$$

which is the error in the hot source temperature value involving also the error in insertion loss measurements.

$$de_c \approx \frac{\partial e_c}{\partial t_{1c}} dt_{1c}$$

$$= -\left(\frac{1 + \tau dt_{cs} - \tau dt_0 + (t_{cs} - t_0)d\tau}{t_0}\right), \tag{28}$$

which is the error in the cold temperature value involving also the error in insertion loss measurements.

$dy = .23(10^{Y/10})dY$—error in the Y factor measurement including effects of repeatability and receiver gain instability.

$d\tau = .23(10^{-A/10})dA$—error in insertion loss measurement.

In computing the error, data was obtained for the paramp which gave the highest noise figure out of the seven S-band paramp subsystems. For example,

$F = 2.19$ db	$t_{hs} = 373°K$	$dt_{cs} = \pm 0.2°K$
$t_{2h} = 368.8°K$	$dt_{hs} = \pm 0.5°K$	$dY = \pm 0.1$ db
$t_{1c} = 90.0°K$	$t_{cs} = 78°K$	$dA = \pm 0.1$ db.

Substituting the above values in the foregoing equations, the final error in the noise-figure measurement as determined by (25) amounts to $dF = \pm 0.1$ db.

B. *Calibration of the Gas Tube with a Hot-Cold Body Standard*

The excess-noise ratio of the gas tube can be written from (17) in decibels as

$$E_{hg} = 4.34 \ln_e\left(\frac{(y' - 1)(t_{hs} - t_{cs})\tau}{c(y - 1)t_0}\right), \tag{29}$$

$$dE_{hg} = 4.34\left(-\frac{dc}{c} + \frac{dy'}{y' - 1} - \frac{dy}{y - 1} + \frac{d(t_{hs} - t_{cs})}{t_{hs} - t_{cs}} + \frac{d\tau}{\tau} - \frac{dt_0}{t_0}\right). \tag{30}$$

Using the same receiver and data as in Section VI-A in addition to the measurement of $y' = 1.31$, the error in the excess-noise ratio for the particular tube is calcu-

lated from above as $dE_{hg} = \pm 0.2$ db. The larger error in the excess-noise ratio of the gas tube as compared to the error in the noise-figure measurement is mainly due to the requirement of two Y-factor measurements in the calibration of gas tubes.

VII. Conclusion

The use of low noise, stabilized parametric amplifier was instrumental in investigating system performance and in the calibration of argon gas tubes under pulsed conditions. The excess-noise ratio of the argon gas tubes under pulsed conditions were found to be on the average 15.7 db at 9.25 Gc, 15.8 db at 2.295 Gc, 15.9 db at 1.3 Gc, and 16.0 db at 0.96 Gc. The cold and hot insertion losses were, respectively, lower and higher at L band in comparison with those at S band. This appears to be consistent with the higher excess-noise ratio obtained at L band than at S band.

The physical position of the tube in this case appeared to have a critical effect on the coupling, consequently affecting the excess-noise ratio of the gas tube. Variations as much as 1 db were measured when the gas tubes were interchanged in different mounts.

Extensive tests with varying conditions gave repeatable results with consistent accuracy, and these results are reiterated for summary purpose.

1) Verification of the standard cold load temperature at $77.5° \pm 0.2°$K when the load was cooled with liquid nitrogen.

2) Consistency in low noise-figure measurements with noise power at different temperatures injected into the system. Noise figures of 1.2, 1.6, and 4.5 db were measured for L, S, and X band, respectively.

3) Agreement between the characteristic temperature of ice water and its measured value by the Y factor method which involved the measured excess-noise ratio of the argon gas tube. Agreement was also obtained between the physical temperature measurement and measurement by Y factor method for the mixture of acetone and dry ice.

Appendix

Mismatches: The following analysis applies only in proximity of the center of a relatively narrow band-pass region of a linear receiver with no spurious responses. Assumption made is that various reflection coefficients involved in the system are essentially constant over the concerned bandwidth. Essentially, the problem amounts to deriving parameters τ, c, and a for a mismatched system by treating each noise-contributing source within the system independently. Noise-power contributions at the receiver input can arise essentially from the following sources in the system; namely, main line hot or cold source, gas tube, network loss, paramp circulator termination, and the amplified leakage signal emanating from the paramp towards the antenna. Of the latter two noise contributions, it is the reflected signal entering the paramp which is of direct concern. However, such noise contributions can be neglected if the mismatch looking from the paramp to the antenna is low and the net isolation of the circulator over the paramp gain is large. The following approximation of the first-order effects verifies the negligible amount of temperature reflected.

$$t_{\text{final}} = (t_{\text{in}}\tau_{\text{cir.}} + t_e)G \cdot I \cdot r \cdot \tau_{\text{cir.}} \tag{31}$$

where t_{final} is the final temperature at the paramp input due to the reflection of the signal traveling from the paramp towards the antenna. The signal from the circulator termination is included.

t_{in} = original total signal at paramp input before amplification (100°K).
$\tau_{\text{cir.}}$ = transmission coefficient of the circulator (0.95).
t_e = paramp effective temperature (200°K).
G = paramp gain 20 db.
I = circulator isolation 36 db.
$r = 0.091$ (VSWR = 1.2).

$$t_{\text{final}} = [(100)(0.95) + 200]\ \frac{(100)(0.091)(0.95)}{4000} = 0.6°\text{K}.$$

The various "effective" system coefficients are related to the scattering coefficients for the mismatched system through the following equations. The system depicted by Fig. 2 or 3 is applicable also for the mismatch case. Transmission coefficient (including dissipation and reflection) is given by

$$\tau = \left| \frac{T_2(1 - \Gamma_3\Gamma_g) + T_1T_3\Gamma_g}{(1 - \Gamma_1\Gamma_s)(1 - \Gamma_3\Gamma_g) - T_1^2\Gamma_s\Gamma_g} \right|^2. \tag{32}$$

Coupling coefficient (including reflection):

$$c = \left| \frac{T_1T_2\Gamma_s + T_3(1 - \Gamma_1\Gamma_s)}{(1 - \Gamma_1\Gamma_s)(1 - \Gamma_3\Gamma_g) - T_1^2\Gamma_s\Gamma_g} \right|^2. \tag{33}$$

Reflection coefficient (including dissipation) at receiver input as viewed from the receiver towards antenna:

$$r = \left| \frac{S_{12}^2\Gamma_s(1 - A\Gamma_g) - S_{22}\Delta_1 + S_{32}^2\Gamma_g(1 - B\Gamma_s)}{\Delta_1(1 - \Gamma_{2i}\Gamma_L)} \right|^2. \tag{34}$$

Absorption coefficient:

$$a = (1 - \tau' - c' - r'). \tag{35}$$

The primed coefficients of (35) exclude dissipative effects and are defined below. Γ_s, Γ_g, and Γ_L are reflection coefficients of a complex source, gas tube, and load, respectively.

$$\tau' = \left| \frac{T_2'(1 - \Gamma_3'\Gamma_g) + T_3'c''\Gamma_g}{(1 - \Gamma_3'\Gamma_g)} \right|^2 \tag{36}$$

$$c' = \left| \frac{c''}{(1 - \Gamma_3'\Gamma_g)} \right|^2 \tag{37}$$

$$r' = \left| \frac{\Gamma_2' + \Gamma_g(c'')^2}{1 - \Gamma_3'\Gamma_g} \right|^2 \tag{38}$$

$$T_1 = S_{13} + \frac{S_{12}S_{23}\Gamma_L}{1 - S_{22}\Gamma_L} \tag{39}$$

$$T_2 + S_{21} = \frac{S_{21}S_{22}\Gamma_L}{1 - S_{22}\Gamma_L} \tag{40}$$

$$T_3 = S_{23} + \frac{S_{23}S_{22}\Gamma_L}{1 - S_{22}\Gamma_L} \tag{41}$$

$$T_2' = S_{12} + \frac{S_{11}S_{12}\Gamma_S}{1 - S_{11}\Gamma_S} \tag{42}$$

$$T_3' = S_{13} + \frac{S_{11}S_{13}\Gamma_S}{1 - S_{11}\Gamma_S} \tag{43}$$

$$\Gamma_1 = S_{11} + \frac{S_{12}^2\Gamma_L}{1 - S_{22}\Gamma_L} \tag{44}$$

$$\Gamma_3 = S_{33} + \frac{S_{23}^2\Gamma_L}{1 - S_{22}\Gamma_L} \tag{45}$$

$$\Gamma_2' = S_{22} + \frac{S_{12}^2\Gamma_S}{1 - S_{11}\Gamma_S} \tag{46}$$

$$\Gamma_3' = S_{33} + \frac{S_{13}^2\Gamma_S}{1 - S_{11}\Gamma_S} \tag{47}$$

$$c'' = S_{32} + \frac{S_{12}S_{13}\Gamma_S}{1 - S_{11}\Gamma_S} \tag{48}$$

$$A = \frac{\begin{vmatrix} S_{12} & S_{13} \\ S_{32} & S_{33} \end{vmatrix}}{S_{12}} \tag{49}$$

$$B = \frac{\begin{vmatrix} S_{11} & S_{12} \\ S_{31} & S_{32} \end{vmatrix}}{S_{32}} \tag{50}$$

$$\Delta_1 = \begin{vmatrix} (1 - S_{11}\Gamma_S) & S_{13}\Gamma_S \\ S_{31}\Gamma_g & (1 - S_{33}\Gamma_g) \end{vmatrix} \tag{51}$$

$$\Gamma_{2i} = \frac{\begin{vmatrix} (1 - S_{11}\Gamma_S) & -S_{12}\Gamma_S & -S_{13}\Gamma_S \\ S_{21} & S_{22} & S_{23} \\ -S_{31}\Gamma_g & -S_{32}\Gamma_g & 1 - S_{33}\Gamma_g \end{vmatrix}}{\Delta_1}. \tag{52}$$

The above equations simplify considerably when high directivity couplers with large coupling factor are used. Note that when Γ_S, Γ_L, Γ_g, $r' = 0$, matched conditions are realized or

$$\tau = \tau' = S_{21}^2, \qquad c = c'' = S_{23}^2,$$

and

$$a = 1 - \tau - C,$$

since

$$r = r' = 0.$$

Calculations for the mismatch case requires phase information and without such information only the limits of the worst possible errors can be obtained by appropriate choice of signs for the various reflection coefficients. For the following sample calculation the variables were assigned with arbitrary phase.

$S_{11} = 0.0385$

$S_{33} = 0.0476$

$S_{32}^2 = 0.0085$ (20.7 db)

$S_{21}^2 = 0.9462$ (0.24 db)

$\Gamma_L = 0.0909$ (VSWR = 1.2)

$\Gamma_s = 0.0385$ (VSWR = 1.08)

$S_{22} = 0.0654$

$\Gamma_g = 0.2$ (VSWR = 1.5)

$S_{31} = 0.005$ (coupling plus directivity = 46 db).

By substitution of the above values in (31)–(52), the following values are obtained:

$\tau = 0.9669$, $c = 0.0086$, $a = 0.0318$, and $r = 0.001$.

With reference to Fig. 2, the gas tube was unfired and the switch was operated for hot and cold load positions. The Y factor measured was 3.56 db.

$$t_{2h} = t_{hs}\tau + t_{cg}c + t_n a + t_{\text{cir.}}r = 372.9^\circ\text{K}$$

$$t_{1c} = t_{cs}\tau + t_{cg}c + t_n a + t_{\text{cir.}}r = 87.7^\circ\text{K}$$

where $t_{hs} = 373^\circ$K, $t_{cs} = 78^\circ$K, $t_n = t_{\text{cir.}} = 297^\circ$K, and $y = 2.27$

$$t_e = \frac{t_{2h} - yt_{1c}}{y - 1} = 148.7^\circ\text{K}$$

which corresponds to a noise figure of $F = 1.8$ db.

Substitution of the above data for an assumed matched system gives the following noise figure: $F = 1.6$ db.

VIII. Acknowledgment

The paramp subsystems were developed for the Jet Propulsion Laboratory (JPL) DSIF contract by the Hughes Aerospace Microwave Components Department under the direction of J. R. Hall (JPL) and Drs.

H. T. Ozaki and J. S. Honda (Hughes). Much gratitude is expressed to them and to their respective staff members. B. L. Walsh, Jr., R. L. Reaser and the members of the Microwave Components Department were instrumental in the successful completion of the program with the Hughes Primary Standards Laboratory participating in the measurement phase. The authors wish to acknowledge also the interest and support of R. O. Hargrove, H. Suyematsu, H. Schiller, L. Shameson (Hughes), and J. Minck and P. Spahn (Hewlett-Packard Company). The discussions with G. Engen of the National Bureau of Standards on power stabilization technique were invaluable and much apppreciated. Thanks are due to Mmes. C. Bottjer, T. Berry and K. Fleming for their indispensable technical services.

IX. References

[1] J. E. Sees, "Fundamentals in Noise Source Calibrations at Microwave Frequencies," Naval Res. Lab., Washington, D. C., Rept. 5051; 1958.
[2] J. S. Wells, W. C. Daywitt, and C. K. S. Miller, "Measurement of effective temperatures of microwave noise sources," 1962 IRE International Convention Record, pt. 3, pp. 220–230.
[3] A. J. Estin, C. L. Trembath, J. S. Wells and W. C. Daywitt, "Absolute measurement of temperatures of microwave noise sources," IRE Trans. on Instrumentation, vol. I-9, pp. 209–213; 1960.
[4] J. Minck and M. Negrete, "Continuous Monitoring of Radar Noise Figures," Hewlett-Packard Co., Palo Alto, Calif., Application Note 43; May 12, 1960.
[5] H. C. Poulter, "An Automatic Noise Figure for Improving Microwave Device Performance," and B. M. Oliver, "Noise Figure and Its Measurement," *Hewlett-Packard J.*, vol. 9, pp. 1–8; January, 1958.
[6] N. J. Kuhn and M. R. Negrete, "Gas discharge noise sources in pulsed operation," 1961 IRE International Convention Record, pt. 3, pp. 166–173.
[7] R. H. Dicke, "The measurement of thermal radiation at microwave frequencies," *Rev. Sci. Instr.*, vol. 17, pp. 268–275; July, 1946.
[8] K. W. Olson, "Reproducible gas discharge noise sources as possible microwave noise standards," IRE Trans. on Instrumentation, vol. I-7, pp. 315–318; December, 1958.
[9] W. W. Mumford, "A broad-band microwave noise source," *Bell Sys. Tech. J.*, vol. 28, pp 608–618; October, 1949.
[10] H. T. Friis, "Noise figures of radio receivers," Proc. IRE, vol. 32, pp. 419–422; July, 1944.
[11] D. O. North, "The absolute sensitivity of radio receivers," *RCA Rev.*, vol. 6, pp. 332–344; January, 1942.
[12] J. P. Gordon and L. D. White, "Noise in maser amplifiers—theory and experiment," Proc. IRE, vol. 46, pp. 1588–1594; September, 1958.
[13] J. K. Hunton, "Analysis of Microwave Measurement Techniques by Means of Signal Flowgraphs," Hewlett-Packard Co., Palo Alto, Calif., Application Note 38; 1960.
[14] R. W. Beatty, "Magnified and squared VSWR responses for microwave reflection coefficient measurements," IRE Trans. on Microwave Theory and Techniques, vol. MTT-7, pp. 346–350; July, 1959.
[15] R. W. Beatty, "Mismatch errors in the measurement of ultra-hi-freq. and microwave variable attenuators," *J. Res. NBS*, vol. 52, pp. 7–9; January, 1954.

Frequency-Selective Limiting*

K. L. KOTZEBUE†, member, ire

Summary—**In the usual microwave limiter, the presence of one or more large signals above a certain threshold level produces a limiting action which can be explained as a change in insertion loss of the limiter so as to maintain a constant output power, regardless of the number of independent signals present. Experimental results of coincidence mode passive ferrite limiters in *S* band and *C* band are presented which show that they do not behave in this manner, but rather to a good approximation limit on a frequency-by-frequency or frequency-selective basis. A qualitative explanation of this phenomenon is presented, using the passive parametric limiter as a model.**

Introduction

THERE ARE MANY occasions where the performance of an electronic system can be improved by the utilization of passive low-power microwave limiters. Protection from burn-out in a sensitive receiver is one application which is well known. A limiter can also find use as a power-leveling device. For example, amplitude variations from a microwave oscillator could be suppressed by utilizing such a limiter at the oscillator output. If the limiter is free of phase distortion, it would be useful in preventing AM-to-PM conversion in systems employing frequency modulation.

An idealized limiter can be characterized as a linear device below a certain threshold value, and a constant output device above this threshold. Illustrated in Fig. 1 is such an idealized characteristic of a power limiter. Below threshold this device has constant loss; above threshold it has constant output power and hence an attenuation which increases in direct proportion to the input power level.

One type of microwave limiter which has proved to be practical for low-power limiting makes use of nonlinear effects in ferrimagnetic material. A typical limiter of this class utilizes the so-called coincidence mode of limiting which Suhl[1] has shown to result in exceedingly low threshold levels. It is the purpose of this paper to report on some recent investigations which have been made on the limiting characteristics of such coincidence mode limiters in the presence of multiple signals within the pass band of the device.

* Received June 4, 1962.
† Watkins-Johnson Company, Palo Alto, Calif.

[1] H. Suhl, "The nonlinear behavior of ferrites at high microwave signal levels," Proc. IRE, vol. 44, pp. 1270–1284; October, 1959.